MOLECULAR PHYSICS, 10 July 2003, VOL. 101, NO. 13, 1983–1995

Taylor & Francis
Taylor & Francis Group

Ab initio calculation of the refractivity and hyperpolarizability second virial coefficients of neon gas

CHRISTOF HÄTTIG[1], JAVIER LÓPEZ CACHEIRO[2], BERTA FERNÁNDEZ[2], and ANTONIO RIZZO[3]*

[1]Forschungszentrum Karlsruhe, Institute of Nanotechnology,
PO Box 3640, D-76021 Karlsruhe, Germany
[2]Department of Physical Chemistry, Faculty of Chemistry,
University of Santiago de Compostela,
E-15782 Santiago de Compostela, Spain
[3]Istituto per i Processi Chimico-Fisici del Consiglio Nazionale delle Ricerche,
Area della Ricerca, via G. Moruzzi 1, loc. S. Cataldo, I-56124 Pisa, Italy

(*Received 23 October 2002; accepted 1 February 2003*)

Second virial coefficients for the density dependence of a number of electric properties are calculated for neon gas. Employing an accurate CCSD(T) potential for the Ne_2 van der Waals dimer and interaction-induced electric dipole polarizabilities and hyperpolarizabilities obtained from CCSD response theory, we evaluated the dielectric, refractivity, Kerr and ESHG second virial coefficients using both a semiclassical and a quantum statistical approach. The results cover a wide range of temperatures and are expected to be more reliable than the available experimental and empirical data. Quantum effects are found to be important only for temperatures below 100 K. The frequency-dependence of the refractivity virial coefficient is found to be small, but not negligible. For frequencies in the visible region it accounts for a few percent of the final results. For the ESHG virial coefficient of neon, frequency dependence is found to be very important, accounting for 20–25% of the second virial coefficient at the typical frequencies employed in experiments.

1. Introduction

In previous work [1–6] we carried out accurate theoretical studies of the second virial coefficients for a number of electric and magnetic properties of helium and argon gases. These coefficients describe the second-order contribution to the pressure dependence of properties caused by pair interactions in the gas phase. In a semiclassical approximation [7] second virial coefficients for properties are in general obtained as integrals over the intermolecular (or interatomic) coordinates of the interaction-induced contribution to the properties weighted by a Boltzmann factor, which is calculated from the interaction potential. Within the semiclassical approximation the calculation of second virial coefficients is thus in principle a simple task once accurate data or reliable models are available for the potential and the interaction-induced properties. The latter are, however, difficult to obtain from experimental data [8, 9]. Additionally, the *ab initio* calculation of interaction-induced properties is a non-trivial problem, particularly if frequency-dependent or nonlinear properties are involved, as for the refractivity and the hyperpolarizability virial coefficients. To obtain accurate results for such properties, highly correlated wavefunctions and large one-particle basis sets must be employed, making the calculation of the properties computationally expensive.

The semiclassical approximation becomes exact in the limit of high temperatures and is often a good approximation to a quantum statistical treatment at and even below room temperature. However, for very low temperatures and for light molecular (or atomic) systems, quantum effects contribute significantly to the virial coefficients and must be accounted for to obtain accurate results. A fully quantum statistical approach requires the calculation of the expectation values of the interaction-induced properties for the rovibrational bound and—even more important—continuum states of the dimer [4]. Depending on the vibrational spectrum of the van der Waals complex and the occurrence of quasi-bound states or resonances in the continuum, the evaluation of the required Slater sums can become a challenging task [4].

In previous publications [1–4] we studied, with helium and argon, two very different prototype systems.

*Author for correspondence. e-mail: rizzo@ipcf.cnr.it: Web http://www.icqem.pi.cnr.it/rizzo/ar.html

Molecular Physics ISSN 0026–8976 print/ISSN 1362–3028 online © 2003 Taylor & Francis Ltd
http://www.tandf.co.uk/journals
DOI: 10.1080/0026897031000109374

For helium gas, a full quantum statistical treatment is essential for the calculation of second virial coefficients for low temperatures, because of its low atomic mass and the low boiling point. Moszynski *et al.* [10, 11] have shown that for helium the perturbative treatment of quantum effects diverges at low temperatures and thus cannot be applied. However, since the He_2 dimer is only very weakly bound, its rovibrational spectrum does not include narrow quasi-bound states and the Slater sums required in the quantum statistical approach can easily be calculated with good accuracy. Conversely, the Ar_2 dimer has a much deeper potential and its rovibrational spectrum contains numerous quasi-bound states [4]. Some of them give rise to very narrow resonances, which results in a difficult integration procedure. This makes an accurate evaluation of the Slater sums rather cumbersome. Due to its larger atomic weight and the higher boiling point, the quantum effects on the second virial coefficients of argon gas are very small—negligible compared to errors caused by the remaining basis set and correlation errors in the *ab initio* calculation of the interaction-induced properties.

Here we present the results of an investigation of second virial coefficients for the electric properties of neon gas as an example of an intermediate case, where quantum effects are expected to be small but non-negligible. Results are reported for the semiclassical approximation and for a full quantum statistical approach. Besides the comparison with experiment, an important aspect of the present study is to obtain some insight into the accuracy of the semiclassical approximation for different molecular weights and depths of the van der Waals potential.

Only few experimental data for second virial coefficients of neon gas are present in the literature. The gas virial coefficient was determined experimentally by Gibbons [12] and by Dymond and Smith [13] for temperatures ranging from 44 to 550 K. Many authors have used these results to check the quality of the intermolecular potentials. Employing an *ab initio* potential curve Eggenberger *et al.* [14] evaluated, among other thermodynamic properties, the gas second virial coefficient for the same temperature range. The authors found quantum effects to be smaller than or comparable in size to the experimental error ($\pm 1\,cm^3\,mol^{-1}$) for temperatures down to about 60 K. However, the deviations were found to increase with decreasing temperature when compared to the available experimental data.

The interaction-induced polarizabilities of Ne_2 have been studied by many authors, mainly theoretically using empirical or *ab initio* data. The results of these studies are far from being satisfactory. Frommhold and Proffitt [15] studied the collision-induced Raman spectra of neon and found the dipole–induced dipole (DID) model for the polarizability anisotropy to be inconsistent with the experimental results. Interaction-induced polarizability anisotropies from quantum chemical calculations gave even worse agreement [16]. The authors claimed their calculations to be too inaccurate.

Dacre evaluated the neon pair polarizability using the configuration interaction (CI) method. He found that the dielectric second virial coefficient calculated from these results ($-0.15\,cm^6\,mol^{-2}$) did not agree well with the available experimental data [17, 18]. A comparison with an empirical model for the pair polarizability anisotropy, derived by Meinander *et al.* [19] from moment analysis in depolarized light scattering experiments, gave for neon an agreement not as good as that found for other noble gases. Ceccherini *et al.* [20] obtained a model for the interaction-induced polarizability that allowed the reproduction of the available measurements of the interaction-induced binary depolarized Raman spectra. When compared with the *ab initio* results [17], deviations attributed to the inaccuracy of the *ab initio* calculations and the experimental data were found.

Maroulis quite recently reported the results of a study of static interaction (hyper)polarizabilities of several systems, including the neon dimer. The author used a finite many-body perturbative approach and coupled cluster (CC) theory [21]. Very recently his studies also extended to mixed dimers (i.e. NeAr) [22]. In [21] the author employs a $7s5p4d1f$ basis set and shows that the effect of triple excitations, as shown by the comparison between the results of a CC singles and doubles (CCSD) approach and those obtained using a CCSD wavefunction with a perturbative treatment of triple excitations (CCSD(T)), is non-negligible—on the order of a few percent, although the size of the basis set is not sufficient to allow for definitive conclusions.

Experimentally, the dielectric second virial coefficient of neon has been determined by Orcutt and Cole [23] at 323 K. The value is $(-0.30 \pm 0.10)\,cm^6\,mol^{-2}$. The authors pointed out that for all the six gases they studied the coefficients are less than those predicted at that time by theories of fluctuations and pair polarizabilities. Vidal and Lallemand [24] determined at 298.15 K a value of $(-0.24 \pm 0.04)\,cm^6\,mol^{-2}$ whereas Huot and Bose [25] measured values of (0.07 ± 0.02), (-0.10 ± 0.30) and $(-0.12 \pm 0.06)\,cm^6\,mol^{-2}$ at 77.4, 242.95 and 323.15 K, respectively. When trying to reproduce the experimental behaviour theoretically, all attempts failed. In the most recent reference in the literature, Bulanin *et al.* [26] calculated the coefficients for a wide range of temperatures using HFD interaction potentials and the CI results taken from the work of Dacre [17, 18]. With these data it was not possible

to reproduce the experimental temperature dependence of the coefficient. Also, theoretical predictions based on the DID model or an empirical model developed by Meinander [27], which accounts also for short-range effects, are in disagreement with measurements carried out, e.g. by Burns *et al.* [28] and by Achtermann *et al.* [29], for the second refractivity virial coefficient of neon.

In the next section we present the results of accurate coupled cluster calculations for the potential and for the frequency-dependent interaction-induced polarizability and hyperpolarizability of the Ne_2 van der Waals dimer. In section 3 these results are employed to evaluate refractivity, Kerr and electric field-induced second harmonic generation (ESHG) second virial coefficients, using both the semiclassical approximation and a quantum statistical approach. In the last section we give some concluding remarks.

2. *Ab initio* calculation of the potential and the interaction-induced (hyper)polarizability

For the present investigation we use an approach similar to that adopted in our previous work on argon and helium [1, 2]. Both the interaction potential and the interaction-induced properties are calculated using size-consistent coupled-cluster methods and the counterpoise correction proposed by Boys and Bernardi [30] to account partially for basis set superposition errors. The latter correction can be formulated for a general size-extensive property P in the case of a homonuclear dimer as

$$\Delta P(R) = P_{A-A}(S_{A-A}|R) - 2P_A(S_{A-A}|R), \qquad (1)$$

where $P_{A-A}(S_{A-A}|R)$ is the property of the dimer evaluated in the dimer basis set S_{A-A} at the interatomic distance R and $P_A(S_{A-A}|R)$ is the property of the monomer evaluated in the dimer basis set for the same geometry.

The potential of the Ne_2 dimer has been investigated previously by several authors using a large variety of methods and basis sets. A number of very accurate potential curves have been published in the literature [31–35]. Most of them are, however, only available close to the equilibrium distance, located at $r_e \approx 310$ pm, which provides insufficient information for the calculation of virial coefficients. Therefore, we computed the Ne_2 potential using the CCSD(T) model and the d-aug-cc-pV5Z basis set [36–40] for 33 interatomic distances ranging from 3 to 30 bohr (158.75 to 1587.5 pm). These calculations were carried out using the coupled cluster program developed by Koch *et al.* [41–43]. The same potential has been used recently by Halkier *et al.* [44] in a study of the nuclear quadrupole coupling constant of ^{21}Ne and it was shown to give an accurate description of the van der Waals interaction with $r_e = 310.5$ pm and $D_e = 127.9\,\mu E_h$ (or 40.40 K) close to the highly accurate results by Gdanitz of 310.07 pm and $131.5\,\mu E_h$, respectively [35]. A HFD-B-like [45] analytic function was then employed to fit the *ab initio* calculated points

$$V(R) = \frac{\epsilon}{k_B} V^*(Ra_0/r_m), \qquad (2)$$

$$V^*(r) = A^* \exp(-\alpha^* r + \beta^* r^2) - F(r) \sum_{n=0}^{2} \frac{c_{6+2n}}{r^{6+2n}}, \qquad (3)$$

$$F(r) = \begin{cases} \exp\left(-(D/r-1)^2\right), & \text{for } r \le D, \\ 1, & \text{for } r \ge D. \end{cases} \qquad (4)$$

The parameters ϵ, α^*, β^*, r_m, c_6, c_8 and c_{10} were determined by a weighted least-squares fit; the multiplicative constant A^* and the parameter D were taken from [45]. The original points are listed in table 1 for some selected internuclear distances, whereas the values of the parameters are given in table 2.

As in [2], to give a measure of the quality of the potential energy curve we computed the second gas virial coefficient $B(T)$, which in the classical approach is given by the expression

$$B(T) = -2\pi N_A \int_0^\infty \left(\exp\left(-V(R)/k_B T\right) - 1\right) R^2 \, dR, \qquad (5)$$

whose validity is limited to temperatures high enough for quantum effects to be negligible. k_B is the Boltzmann constant. The results obtained by integrating the

Table 1. Ne_2 potential calculated at the CCSD(T)/d-aug-cc-pV5Z level.

R/bohr	$V(R)/\mu E_h$
3.0	91163.5497
3.7	15519.8232
4.7	827.3348
5.15	64.0232
5.3	−29.5414
5.5	−95.9638
5.8	−127.0377
6.0	−125.4761
6.5	−97.3739
7.0	−67.2280
8.0	−30.2824
10.0	−7.3516
15.0	−0.5917
20.0	−0.1023
30.0	−0.0087

Table 2. Parameters of the weighted least-squares fits of the CCSD(T)/d-aug-cc-pV5Z potential for Ne_2 to a HFD-B-like function, equations (2)–(4). The values of the parameters are given for R in bohr and $V(R)$ in hartree; the conversion from hartree to K (i.e. the Boltzmann constant in atomic units) was taken as $315\,773.0\,K\,E_h^{-1}$.

Parameter	Value
A^*	895717.95
α^*	12.041788
β^*	−0.2289419
c_6	2.6178124
c_8	1.5141754
c_{10}	0.5777010
r_m	2.768605 Å
D	1.36
ϵ/k_B	36.895522 K

Table 3. The gas second virial coefficient B(T) (in $cm^3\,mol^{-1}$). Semiclassical results and comparison with experimentally available data.

T/K	This work	Exp.	Ref.
44	−46.36	−46.1	[12]
50	−36.02	−35.4	[12]
60	−24.33	−24.9	[12]
70	−16.58	−17.1	[12]
80	−11.10	−12.8	[13]
100	−3.89	−6.0	[13]
125	1.45	−0.4	[13]
150	4.78	3.2	[13]
200	8.60	7.7	[13]
250	10.65	10.0	[13]
300	11.88	11.3	[13]
350	12.66	12.1	[13]
400	13.17	12.7	[13]
450	13.52	13.1	[13]
500	13.76	13.4	[13]
550	13.92	13.7	[13]

analytic function given above between 0.1 and 500 bohr are given and compared to available experimental data in table 3 and in figure 1. The agreement between our estimates and experiment is fair for all temperatures, which suggests that quantum effects are probably small for this property down to 40 K. The sensitivity of the semiclassical integral in equation (5) to the features of the potential and the important role that regions of very low interatomic distances maintain in the determination of $B(T)$ have been discussed in [2].

Since the virial coefficients are—at least for noble gases—only weakly frequency dependent [1, 3], the dispersion of the interaction-induced properties was

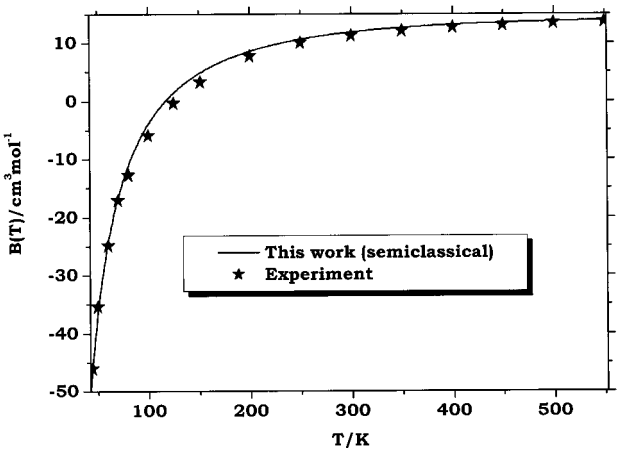


Figure 1. Temperature dependence of the gas second virial coefficient. Comparison is made with previously available results.

approximated to second order in the frequency as

$$\Delta\alpha(-\omega;\omega) = \Delta\alpha + \omega^2\Delta S(-4) + \mathcal{O}(\omega^4), \quad (6)$$

$$\Delta\gamma_{||}(\Omega) = \Delta\gamma_{||} + \omega_L^2\,\Delta(\gamma_{||}\times A) + \mathcal{O}(\omega_i^4), \quad (7)$$

$$\Delta\gamma_K(\omega;0,0,\omega) = \Delta\gamma_{||} + \omega^2\Delta D_K(2) + \mathcal{O}(\omega^4), \quad (8)$$

with Ω employed here and below as a shorthand notation for the sequence $\omega_0;\omega_1,\omega_2,\omega_3$ and $\omega_L^2 = \omega_0^2+\omega_1^2+\omega_2^2+\omega_3^2$. This reduces the computational efforts considerably and it leads to virial coefficients which are also correct through $\mathcal{O}(\omega^2)$. In addition to the static interaction polarizability—both the isotropic part $\Delta\alpha_{ave}$ and the anisotropy $\Delta\alpha_{ani}$—and the hyperpolarizability $\Delta\gamma_{||}$, the interaction-induced Cauchy moments $\Delta S(-4)$ and the dispersion coefficients for the isotropic and the dc-Kerr hyperpolarizability $\Delta(\gamma_{||}\times A) = \Delta D_{||}(2)$ and $\Delta D_K(2)$ are thus needed. At the CCSD response level these properties and dispersion coefficients are available analytically (i.e. without employing fits) using the program described in [46–49], which is available in the DALTON 1.2 package [43]. These calculations were carried out for 32 interatomic distances between 3 and 20 bohr and employed the d-aug-cc-pVQZ basis set of Dunning and co-workers [36–40], augmented with a $(3s3p2d1f1g)$ set of diffuse midbond functions [1, 3, 50, 51]. The resulting basis set is denoted in the following as d-aug-cc-pVQZ-33211. An investigation carried out at $R = 5.0$ au (see table 4) indicates that with the d-aug-cc-pVQZ-33211 basis the interaction-induced polarizabilities and hyperpolarizabilities are obtained within a few percent of the CCSD basis set limit. To interpolate the interaction properties between the calculated points, analytic functions were fitted to the *ab initio* results. A selection

of the original points are reported in table 5, whereas the fitting functions and the parameters are given in table 6.

In figures 2 to 4 the present results for the interaction properties are compared with the latest available empirical functions. For the interaction-induced isotropic polarizability we compare the present results with those obtained by Frommhold and Proffitt using the data obtained from the polarized Raman spectrum [15]. The parameters for the function (see equation (16) in [15]) were taken as $\lambda_t^* = 135\,a_o^3$, $r_t = 0.626\,a_o$ and $A_6 = 224\,a_o^9$, corresponding to the set that gave the best agreement with respect to the spectral results. The empirical function shows a steeper decrease than the *ab initio* calculated curve in the region of short R values, whereas the agreement for long interatomic distances is good (figure 2). We also compare to the results of Frommhold and Proffitt for the anisotropic contribution, obtained from the depolarized Raman spectrum [15]. The parameters for the function (equation (11) in [15] in this case) were taken as $\lambda^* = 720\,a_o^3$, $r_o = 0.509\,a_o$

Table 4. Basis set convergence of the CCSD results for the interaction-induced polarizabilities $\Delta\alpha_{ave}$, $\Delta\alpha_{ani}$ and hyperpolarizabilities $\Delta\gamma_{||}$, $\Delta\gamma_{\perp}$. The calculations have been carried out at $R = 5.00$ bohr. The results are given in atomic units (au).

Basis Set	$\Delta\alpha_{ave}$	$\Delta\alpha_{ani}$	$\Delta\gamma_{||}$	$\Delta\gamma_{\perp}$
d-aug-cc-pVDZ-33211	0.0358	−0.2473	15.8325	5.2775
d-aug-cc-pVTZ-33211	0.0292	−0.2415	9.4955	3.1652
d-aug-cc-pVQZ-33211	0.0281	−0.2389	9.3566	3.1189
d-aug-cc-pV5Z-33211	0.0277	−0.2379	9.4075	3.1358

Table 6. Parameters of the weighted least-squares fits to the interaction-induced properties. The fit functions have been chosen as follows: $P(R) = -\exp(-(R-s)^2/\rho) + \sum_{n=0}^{3} A_{6+2n}R^{-6-2n}$ for $\Delta\alpha_{ave}$ and $\Delta S_{ave}(-4)$; $P(R) = -\exp(-(bR^3 + R - s)/\rho) + A_3R^{-3} + \sum_{n=0}^{2} A_{6+2n}R^{-6-2n}$ for $\Delta\alpha_{ani}$ and $\Delta S_{ani}(-4)$, and $P(R) = D\{[1-(1+bR+cR^2)\exp(-a(R-r))]^2 - 1\} + \exp(1-\exp[-a(R-er)])A_6R^{-6}$ for $\Delta\gamma_{||}$, $\Delta D_{||}(2)$ and $\Delta D_K(2)$.

	$\Delta\alpha_{ave}$	$\Delta S_{ave}(-4)$	
s	0.783255	1.87398	
ρ	5.34016	5.13093	
A_6	297.685	1244.76	
A_8	−6905.68	−36669.9	
A_{10}	59806.0	376798	
A_{12}	−151689	−1139134	
	$\Delta\alpha_{ani}$	$\Delta S_{ani}(-4)$	
b	8.00900×10^{-3}	13.1712×10^{-3}	
s	3.80920	5.31723	
ρ	0.986526	1.50426	
A_3	40.9336	88.2682	
A_6	105.888	631.809	
A_8	6125.93	3698.18	
A_{10}	−28987.1	0.	
	$\Delta\gamma_{||}$	$\Delta D_{||}(2)$	$\Delta D_K(2)$
D	33.4726	136.798	131.356
b	−0.950276	−0.534505	−0.639462
c	0.313117	0.144986	0.111701
a	1.69236	1.53458	1.75300
r	3.47856	3.79049	5.00979
e	1.12857	0.973356	0.913738
A_6	55417.2	236713	375150

Table 5. Interaction-induced polarizabilities $\Delta\alpha_{ave}$ and $\Delta\alpha_{ani}$, Cauchy moments $\Delta S_{ave}(-4)$ and $\Delta S_{ani}(-4)$, isotropic hyperpolarizability $\Delta\gamma_{||}$ and hyperpolarizability dispersion coefficients $\Delta D_{||}(2)$ and $\Delta D_K(2)$ as a function of the internuclear distance R calculated at the CCSD/d-aug-cc-pVQZ-33211 level. All values given in au.

R	$\Delta\alpha_{ave}$	$\Delta S_{ave}(-4)$	$\Delta\alpha_{ani}$	$\Delta S_{ani}(-4)$	$\Delta\gamma_{||}$	$\Delta D_{||}(2)$	$\Delta D_K(2)$
3.00	−0.31554	−0.42553	0.28010	1.01960	14.5927	166.764	345.166
3.50	−0.22391	−0.51976	0.21375	0.26831	−15.6518	−21.0307	−39.6770
4.00	−0.12894	−0.38192	0.24078	0.21884	−17.9822	−49.7398	−99.2923
4.50	−0.06440	−0.23332	0.25306	0.29131	−14.1495	−46.2748	−93.2433
5.00	−0.02814	−0.12446	0.23892	0.34408	−9.35690	−34.5483	−70.0892
5.50	−0.01044	−0.05849	0.20944	0.35229	−5.41368	−22.5601	−46.0781
6.00	−0.00282	−0.02360	0.17594	0.32803	−2.75407	−13.1938	−27.1574
7.00	0.00081	−0.00047	0.11856	0.24598	−0.38196	−3.14428	−6.66690
8.00	0.00073	0.00225	0.08050	0.17319	0.14906	−0.06507	−0.30548
10.00	0.00023	0.00094	0.04115	0.08925	0.12556	0.42641	0.79582
12.00	0.00009	0.00035	0.02377	0.05143	0.05314	0.19417	0.36394
14.00	0.00004	0.00015	0.01495	0.03228	0.02251	0.08331	0.15744
16.00	0.00001	0.00005	0.01000	0.02156	0.00853	0.03331	0.06390
18.00	0.00001	0.00002	0.00701	0.01511	0.00299	0.01214	0.02360
20.00	0.00000	0.00001	0.00511	0.01101	0.00108	0.00428	0.00852

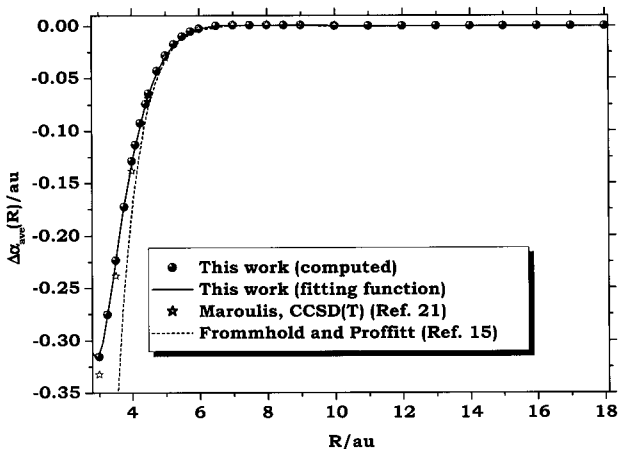


Figure 2. Interaction-induced static isotropic polarizability in terms of R and the analytical function fitted to it (see text). The empirical curve obtained by Frommhold and Proffitt [15] is also plotted, together with the CCSD(T) results of Maroulis, see [21].

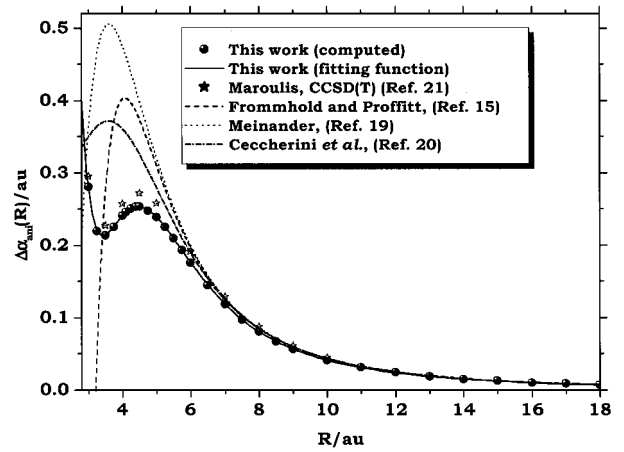


Figure 3. Interaction-induced static anisotropic polarizability in terms of R and the analytical function fitted to it (see text). The empirical curves obtained by Frommhold and Proffitt [15], Meinander *et al.* [19] and Ceccherini *et al.* [20] are also plotted, together with the CCSD(T) results of Maroulis [21].

and $\alpha = 0.3992 \times 10^{-24}\,\mathrm{cm}^3$ (2.6939 au). The agreement with the present results is worse than for the isotropic component, especially in the region of short R distances (dashed curve in figure 3). For the anisotropy in figure 3 we compare also with the empirical function obtained by Meinander *et al.* from the depolarized collision-induced light scattering spectrum [19] (dotted curve, equation (3 *a*) in [19], parameters: $B = 50\,\text{Å}^3$, $\alpha_0 = 0.3989\,\text{Å}^3$ (2.6919 au), $A = 0.664\,\text{Å}^9$, $r_0 = 0.294\,222\,\text{Å}$) and with the results of Ceccherini *et al.* [20] (dashed-dotted curve, equation (12) in [20], parameters: $r_1 = 0.755$ au, $r_0 = 0.8426$ au, $\Gamma = 101$ au, $C_6 = -6.8$ au). The latter

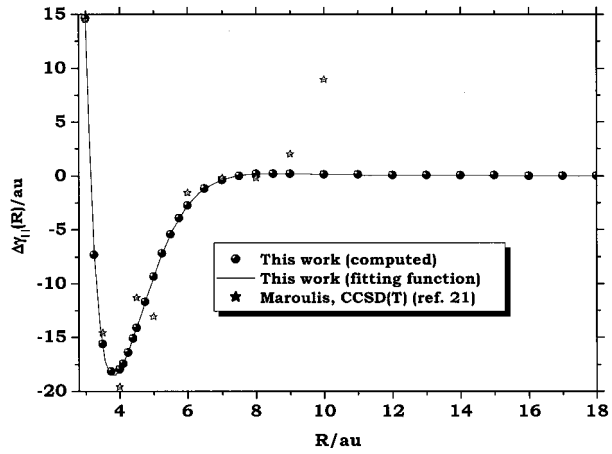


Figure 4. Interaction-induced static isotropic hyperpolarizability in terms of R and the analytical function fitted to it (see text). Also enclosed are the CCSD(T) results of Maroulis [21].

curve gives the best overall agreement with our *ab initio* values.

The results of the recent study by Maroulis [21] are also included in figures 2 to 4. Although the interaction-induced properties were computed employing rather sophisticated methods as CCSD and CCSD(T), the quality of the results is probably still highly influenced by the limited basis set used in [21]. We also note that the effect of linked triple excitations for second hyperpolarizabilities is much larger in the orbital-relaxed finite field coupled cluster method used in these calculations than in the CC response approach adopted in the present work [52]. Maroulis mentions numerical instabilities in the finite field method, and these are more than evident in figure 4, where the average parallel interaction-induced hyperpolarizability as computed in [21] for R between 7 and 10 au shows no intention of adapting to the expected long range R^{-6} pattern.

3. Calculation of the virial coefficients

3.1. *Semiclassical approximation*

Within the semiclassical approximation, the refractivity second virial coefficient is given by the expression [53]

$$B_R(\omega, T) = \frac{N_A^2}{6\epsilon_0} 4\pi \int_0^\infty \Delta\alpha_{\mathrm{ave}}(\omega, R) \times \exp\left(-V(R)/k_B T\right) R^2\,\mathrm{d}R. \qquad (9)$$

The dielectric second virial coefficient $B_\epsilon(T)$ is defined as the static ($\omega = 0$) limit of $B_R(\omega, T)$. Inserting for $\Delta\alpha_{\mathrm{ave}}(\omega, R)$ the expansion in Cauchy moments, equation (6), one obtains [1]:

$$B_R(\omega, T) = B_\epsilon(T) + \omega^2 B_R^{(2)}(T) + \ldots, \qquad (10)$$

where the second-order coefficient $B_R^{(2)}(T)$ is calculated analogous to equation (9), but with $\Delta\alpha_{\rm ave}(\omega, R)$ replaced by $\Delta S_{\rm ave}(-4, R)$. The second Kerr virial coefficient has contributions related to the interaction-induced polarizability anisotropy and to the dc-Kerr hyperpolarizability $\Delta\gamma_{\rm K}(\omega, R)$, respectively

$$B_{\rm K}(\omega, T) = \frac{N_{\rm A}^2}{162\epsilon_0}\left(\frac{1}{5k_{\rm B}T}X_{\rm K}^{\alpha}(\omega, T) + X_{\rm K}^{\gamma}(\omega, T)\right) = B_{\rm K}^{\alpha}(\omega, T) + B_{\rm K}^{\gamma}(\omega, T), \quad (11)$$

with $X_{\rm K}^{\alpha}(\omega, T)$ and $X_{\rm K}^{\gamma}(\omega, T)$ defined as

$$X_{\rm K}^{\alpha}(\omega, T) = 4\pi\int_0^{\infty}\Delta\alpha_{\rm ani}(\omega, R)\Delta\alpha_{\rm ani}(0, R) \times \exp\left(-V(R)/k_{\rm B}T\right)R^2\,{\rm d}R, \quad (12)$$

$$X_{\rm K}^{\gamma}(\omega, T) = 4\pi\int_0^{\infty}\Delta\gamma_{\rm K}(\omega, R) \times \exp\left(-V(R)/k_{\rm B}T\right)R^2\,{\rm d}R. \quad (13)$$

As in [1], $X_{\rm K}^{\alpha}(\omega, T)$ and $X_{\rm K}^{\gamma}(\omega, T)$ are expanded through second order in ω using the relationships equations (6) and (8), but without employing Kleinmann symmetry, in contrast to [1]. Finally, in the semiclassical approximation the second virial coefficient for the isotropic hyperpolarizability $\gamma_{||}(\Omega)$ is obtained as [1, 54]

$$B_{\gamma}(\Omega, T) = \frac{N_{\rm A}}{8\pi\epsilon_0}4\pi\int_0^{\infty}\Delta\gamma_{||}(\Omega, R) \times \exp(-V(R)/k_{\rm B}T)R^2\,{\rm d}R. \quad (14)$$

The frequency dependence of $B_{\gamma}(\Omega, T)$ is again approximated using the expansion equation (7) through second order:

$$B_{\gamma}(\Omega, T) \approx B_{\gamma}^{(0)}(T) + \omega_{\rm L}^2 B_{\gamma}^{(2)}(T), \quad (15)$$

where $B_{\gamma}^{(0)}(T)$ and $B_{\gamma}^{(2)}(T)$ are calculated similar to equation (14), but again with $\Delta\gamma_{||}(\Omega, R)$ replaced by the static interaction-induced hyperpolarizability and by $\Delta\gamma_{||}(0) \times A$, respectively.

To compute the virial coefficients we employed the fits for the Ne_2 potential and for the interaction-induced properties reported in tables 2 and 6, respectively. The required integrals were evaluated by means of numerical quadrature.

3.2. *Quantum statistical calculations*

The quantum statistical expression for the second dielectric virial coefficient was derived in detail by Moszynski and co-workers [10, 11, 55]. In a quantum statistical treatment the average over the semiclassical expression for the pair density $\exp(-V(R)/k_{\rm B}T)$ is essentially replaced by a derivative of the trace of the quantal density operator with respect to external fields, where the derivative taken is the same as that taken from the (quasi-)energy to obtain the respective underlying property of the dimer. Thus the dielectric second virial coefficient is obtained as

$$B_{\epsilon}(T) = \frac{2\pi k_{\rm B}T}{3}\int_0^{\infty}\left(\frac{\partial^2 W(R; F)}{\partial F^2}\right)_{F=0}R^2\,{\rm d}R \quad (16)$$

$$= \frac{2\pi}{3}\int_0^{\infty}W(R, 0)\Delta\alpha_{\rm ave}(R)R^2\,{\rm d}R, \quad (17)$$

where F is the strength of an external homogenous electric field and $W(R, F)$ is the Slater sum [11, 56]:

$$W(R; F) = \lambda_{\rm B}^3\langle R|\exp(-\beta\mathcal{H}(F))|R\rangle + \frac{\lambda_{\rm B}^3(-1)^{2I}}{2I+1}\langle -R|\exp(-\beta\mathcal{H}(F))|R\rangle\,. \quad (18)$$

In the last equation we have introduced the field-dependent Hamiltonian $\mathcal{H}(F) = -(\hbar^2/2\mu)\nabla^2 + V(R) - (1/2)\Delta\alpha_{zz}(\mathbf{R})F^2 + \mathcal{O}(F^3)$, the thermal wavelength $\lambda_{\rm B} = (2\pi\hbar^2/k_{\rm B}T\mu)^{1/2}$ and the nuclear spin quantum number I. The reduced mass is denoted by μ. Inserting the complete set of eigenfunctions of $\mathcal{H}(0)$, corresponding to the bound and continuum rovibrational states of the (unperturbed) dimer, one obtains the expression [11]:

$$B_{\epsilon}(T) = \frac{2\pi\lambda_{\rm B}^3}{3}\sum_{J=0}^{\infty}(2J+1)\left(1+\frac{(-1)^{J+2I}}{2I+1}\right) \times\left[\sum_n\exp\left(-\frac{E_{nJ}}{k_{\rm B}T}\right)\langle\chi_{nJ}(R)|\Delta\alpha_{\rm ave}(R)|\chi_{nJ}(R)\rangle + \int_0^{\infty}\exp\left(-\frac{\hbar^2k^2}{2\mu k_{\rm B}T}\right)\langle\chi_{kJ}(R)|\Delta\alpha_{\rm ave}(R)|\chi_{kJ}(R)\rangle\frac{\mu}{\hbar^2k}{\rm d}k\right], \quad (19)$$

where J is the rotational quantum number and χ_{nJ} (χ_{kJ}) are the radial parts of the bound (continuum) eigenfunctions of the field-independent Hamiltonian. See [4, 11] for details.

A similar approach can also be used for the other second virial coefficients. For some properties, however, additional assumptions have to be made; e.g. if frequency dependence has to be considered [57]. If products of interaction-induced properties contribute, as for example for the Kerr second virial coefficients, the exact quantum statistical expressions become more involved due to the appearance of an extra integration which accounts for the non-vanishing commutator between the Hamiltonian

for the intermolecular motion $\mathcal{H}(0)$ and the interaction-induced properties $\Delta P(R)$ [57, 58]. In such cases it is convenient to introduce the additional assumption that these commutators are negligible. This approximation becomes exact in the classical limit, i.e. for small thermal wavelengths, and it provides an upper bound for $B_K(T)$ [58]. Under these conditions the (approximate) quantum statistical expression for second virial coefficients is obtained by replacing the pair density $\exp(-V(R)/k_BT)$ by the (field-independent) Slater sum $W(R;0)$ in the semiclassical expressions given in section 3.1. For example, the (approximate) expression for the Kerr second virial coefficients is

$$B_K(\omega, T) = \frac{N_A^2}{162\epsilon_0}\left(\frac{1}{5k_BT}X[\Delta\alpha_{ani}(\omega, R)\Delta\alpha_{ani}(0, R), T] + X[\Delta\gamma_K(\omega, R), T]\right), \quad (20)$$

with

$$X[\Delta P(R), T] = 4\pi\lambda_B^3\sum_{J=0}^{\infty}(2J+1)\left(1+\frac{(-1)^{J+2I}}{2I+1}\right) \times\left[\sum_n \exp\left(-\frac{E_{nJ}}{k_BT}\right)\langle\chi_{nJ}(R)|\Delta P(R)|\chi_{nJ}(R)\rangle + \int_0^{\infty}\exp\left(-\frac{\hbar^2k^2}{2\mu k_BT}\right)\langle\chi_{kJ}(R)|\Delta P(R)|\chi_{kJ}(R)\rangle\frac{\mu}{\hbar^2k}\,dk\right]. \quad (21)$$

The evaluation of the quantum statistical expressions for the virial coefficients requires two numerical integrations, one over the interatomic distance R and the other over the wavenumber k, plus an (in principle) infinite summation over the angular momentum J. The summation over n (the bound states supported by the potential of the dimer) ranged in our case from 0 to 2 for the lowest ($J=0$) rotational quantum number, with $D_0 = 15.40\,cm^{-1}$, $D_1 = 2.50\,cm^{-1}$ and $D_2 < 0.03\,cm^{-1}$. Experimentally [59, 60] three stable vibrational levels were detected, with the highest lying very close to the dissociation limit: $D_0 = 16.3\,cm^{-1}$, $D_1 = 2.6\,cm^{-1}$ and $D_2 \leq 0.01\,cm^{-1}$. Cybulski and Toczylowski [33] found two vibrational levels in their *ab initio* study exploiting a CCSD(T) wavefunction and using, among others, an aug-cc-pV5Z basis set supplemented with a set of $3s3p2d2f1g$ midbond functions. The recent study by Gdanitz [35], improving slightly on the potential curve of [33], determines again three vibrational levels for $J=0$ in the neon dimer, with $D_0 = 16.406\,cm^{-1}$, $D_1 = 2.789\,cm^{-1}$ and the third and highest level placed only $0.004\,cm^{-1}$ below the dissociation limit. For the integration over R we used an even-spaced grid ranging from 0.5 to 100 bohr with a step width of 0.0005 bohr for $J < 250$, and a different grid, going from 0.5 to 200 bohr with a step width of 0.0002 bohr for $J \geq 250$. These grids were used both for the solution of the vibrational Schrödinger equation and for the evaluation of the matrix elements $\langle\chi(R)|\Delta P(R)|\chi(R)\rangle$. The atomic mass of Ne was taken as 19.992 4356 amu [61]. For the integration over the wavenumber k an even-spaced grid cannot be applied—at least not for all values of J—since for certain values of J very narrow resonance peaks appear, which require more elaborate integration schemes. We employed the algorithm described in [4], which accounts explicitly for the quasi-bound states and which allows for an accurate and efficient integration of the matrix elements over k. For $J < 250$, this integration was carried out for k from 0.5 to 200 au, whereas for $J \geq 250$ the interval went from 1.0 to 300 au. Finally, the summation over J was carried out up to $J = 500$. These parameters were chosen such that convergence within about 0.01% in the summations was reached. The fact that indeed convergence within this accuracy is reached in the numerical integrations is corroborated by the comparison between quantum statistical and semiclassical results for the higher temperatures, where the latter become exact. The two approaches should give practically identical results, which is what we find within the specified accuracy.

The total errors in the virial coefficients are thus dominated by the errors caused by the limited number of available data points for the potential and the interaction-induced properties and, in particular, by the approximations made in the quantum-chemical calculations, i.e. the incompleteness of the one-electron basis set and the residual electron correlation error.

All calculations for the second virial coefficients were carried out with a modified version of the KORG program [62] originally written by I. Cacelli, and which has been extended for the calculation of second virial coefficients. For the present task we have improved the code such that the fits to the *ab initio* calculated points, reported in section 2, can be used for the calculation of second virial coefficients without employing intermediate spline interpolations.

Conversion factors between au, SI and esu units for the properties presented and discussed in the next section can be found in [3].

4. Results and discussion

4.1. *Dielectric and refractivity second virial coefficients*

The results for the dielectric and refractivity second viral coefficients of neon are given in table 7. Both quantum statistical and semiclassical results are reported and compared to the experimental values

Table 7. The dielectric and refractivity second virial coefficients ($cm^6\,mol^{-2}$).

	Semiclassical		Quantum statistical		Experimental
T/K	$B_\epsilon(T)$	$B_R^{(2)}(T)$	$B_\epsilon(T)$	$B_R^{(2)}(T)$	$B_\epsilon(T)$, $B_R(T)$
40.0	−0.0659	−0.6718	−0.0551	−0.5810	
77.4	−0.0525	−0.4997	−0.0492	−0.4715	0.07 ± 0.02 [25][a]
100.0	−0.0546	−0.4868	−0.0524	−0.4683	
140.0	−0.0614	−0.4948	−0.0600	−0.4841	
180.0	−0.0690	−0.5151	−0.0681	−0.5080	
220.0	−0.0766	−0.5386	−0.0759	−0.5337	
242.95	−0.0808	−0.5525	−0.0803	−0.5485	−0.10 ± 0.03 [25][a]
273.15	−0.0863	−0.5706	−0.0859	−0.5676	
298.15	−0.0906	−0.5853	−0.0903	−0.5830	−0.24 ± 0.04 [24][a]
					−0.14 ± 0.14 [28][b]
					−0.11 ± 0.22 [28][c]
					−0.06 ± 0.09 [63][d]
303.15	−0.0915	−0.5882	−0.0912	−0.5861	−0.11 ± 0.02 [29][e]
323.0	−0.0949	−0.5997	−0.0947	−0.5980	−0.30 ± 0.10 [64][a]
323.15	−0.0949	−0.5998	−0.0947	−0.5981	−0.12 ± 0.06 [25][a]
					−0.22 ± 0.02 [65][a]
370.0	−0.1025	−0.6259	−0.1025	−0.6252	
410.0	−0.1088	−0.6473	−0.1088	−0.6473	

[a] B_ϵ;
[b] $B_R(\lambda = 632.8\,nm)$ at T = 298.2 K;
[c] $B_R(\lambda = 457.9\,nm)$ at T = 298.2 K;
[d] $B_R(\lambda = 632.8\,nm)$ at T = 299 K;
[e] $B_R(\lambda = 632.8\,nm)$; cf. computed $-0.157\,cm^6\,mol^{-2}$.

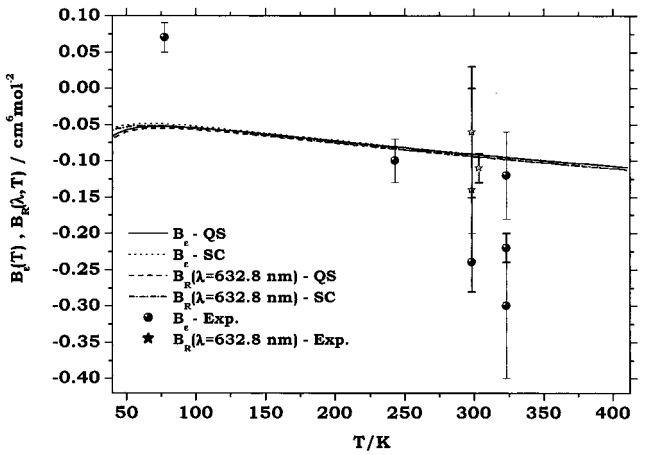


Figure 5. Temperature dependence of the dielectric second virial coefficient $B_\epsilon(T)$—semiclassical (SC) and quantum statistical (QS) contributions—and of the refractivity second virial coefficient $B_R(\omega, T)$ computed at $\lambda = 632.8\,nm$. The available experimental data for $B_\epsilon(T)$ and $B_R(\omega, T)$ are also shown.

available. In figure 5 the data are plotted against the temperature. As anticipated in the introduction, due to the mass of the Ne atom being in between that of helium and argon, the contribution of the quantum effects to the virial coefficient is in between those obtained for helium and argon [4]. Only at temperatures below 100 K do the quantum effects start to be significant (> 5%) for neon. At the experimentally studied temperatures, these effects are negligible and the semiclassical values can be expected to give accurate estimates of the coefficients. Frequency dispersion is also rather weak, being contained between 5% (at low temperatures) and 3% (at high temperatures) for a wavelength of 632.8 nm. The effect of frequency is only slightly more accentuated in the quantum statistical calculations at low temperatures. When comparing with the available experimental data, we can see that, as happened with the helium and argon results [4], the spread of the experimental results is very large and most values have large error bars. This makes any discussion on the supposed agreement or disagreement between theory and experiment quite useless. The experimental datum at 77.4 K carries a probably too optimistic error bar, given the level of accuracy of our study. Therefore, and as concluded also in previous papers devoted to the study of helium and argon, we advocate new experimental determinations which might shed some light on the comparison with the theoretical data. Recent advances in the field are in this respect particularly promising [8].

Table 8. The Kerr second virial coefficients ($V^2\,m^8\,mol^{-2} \times 10^{-35}$). We define $B_K^{\alpha}(\omega, T) = B_K^{(0),\alpha} + \omega^2 B_K^{(2),\alpha}$ and analogously $B_K^{\gamma}(\omega, T) = B_K^{(0),\gamma} + \omega^2 B_K^{(2),\gamma}$, with ω assumed to be given in au.

	Semiclassical				Quantum statistical			
T/K	$B_K^{(0),\alpha}(T)$	$B_K^{(2),\alpha}(T)$	$B_K^{(0),\gamma}(T)$	$B_K^{(2),\gamma}(T)$	$B_K^{(0),\alpha}(T)$	$B_K^{(2),\alpha}(T)$	$B_K^{(0),\gamma}(T)$	$B_K^{(2),\gamma}(T)$
40.00	29.27	56.54	−0.94	−11.08	26.87	51.93	−0.88	−9.66
77.40	11.77	22.76	−0.65	−7.84	11.37	21.97	−0.64	−7.39
100.00	8.68	16.75	−0.62	−7.36	8.47	16.34	−0.61	−7.07
140.00	5.97	11.47	−0.61	−7.07	5.88	11.29	−0.60	−6.90
180.00	4.58	8.75	−0.61	−7.02	4.53	8.65	−0.61	−6.90
220.00	3.73	7.10	−0.63	−7.05	3.70	7.03	−0.63	−6.97
242.95	3.37	6.41	−0.64	−7.09	3.35	6.35	−0.64	−7.03
273.15	3.00	5.68	−0.65	−7.15	2.98	5.64	−0.65	−7.10
274.00	2.99	5.66	−0.65	−7.15	2.97	5.62	−0.65	−7.10
298.15	2.75	5.20	−0.66	−7.21	2.74	5.16	−0.66	−7.17
303.15	2.70	5.11	−0.67	−7.22	2.69	5.08	−0.66	−7.18
323.15	2.54	4.79	−0.67	−7.26	2.53	4.76	−0.67	−7.23
340.00	2.42	4.56	−0.68	−7.30	2.41	4.53	−0.68	−7.28
370.00	2.23	4.19	−0.69	−7.37	2.22	4.16	−0.69	−7.35
410.00	2.01	3.78	−0.71	−7.47	2.01	3.76	−0.71	−7.45

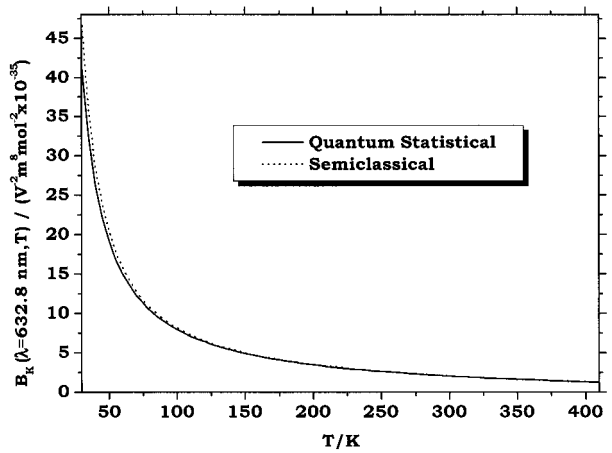


Figure 6. The Kerr second virial coefficient $B_K(\omega, T)$ as a function of the temperature computed at $\lambda = 632.8\,nm$ ($V^2\,m^8\,mol^{-2} \times 10^{-35}$).

4.2. *Second Kerr and ESHG virial coefficients*

The results obtained for the second Kerr virial coefficient $B_K(\omega, T)$ are given in table 8, where the two contributions $B_K^{\alpha}(\omega, T)$ and $B_K^{\gamma}(\omega, T)$ are further split into their static and dispersion parts. Figure 6 shows the behaviour of $B_K(\omega, T)$ for neon for a wavelength of 632.8 nm.

For neon, as for helium, the deviations from linearity found in the experimental work by Buckingham and Dunmur dated 1968 were negligible [66]. A linear fit to the Kerr constant was found to be adequate for densities of more than $10^{-3}\,mol\,cm^{-3}$. To our knowledge, no other experimental studies of the density dependence of the Kerr constant of neon appear in the literature. Our study of [3] shows that in the case of helium the two contributions $B_K^{\alpha}(\omega, T)$ and $B_K^{\gamma}(\omega, T)$ essentially tend to cancel each other at temperatures approaching standard conditions, with their sum $B_K(\omega, T)$ changing sign approximately around room temperature. This behaviour is perfectly in line with the experimental evidence of [66]. The effect does not appear in the case of neon, where, as figure 6 clearly shows, $B_K(\omega, T)$—at least for $\lambda = 632.8\,nm$—decreases smoothly as T increases, remaining positive at least up to 410 K. Here the $B_K^{\alpha}(\omega, T)$ contribution decreases steadily as the temperature increases, whereas $B_K^{\gamma}(\omega, T)$ remains practically unchanged and from 30 times to twice smaller than the other contribution. The effect of pair interactions in neon is thus small but still stronger at room temperature than predicted and observed for helium.

Quantum effects are significant only below 50–60 K, where they decrease the value of $B_K(\omega, T)$ by more than 5%. Above 180 K the difference between quantum statistical and semiclassical results in table 8 is less than 1%. This is also the limit of accuracy of the numerical integration employed for these calculations. Frequency dispersion modifies the static values of $B_K^{\alpha}(\omega, T)$ by ≈2% and those of $B_K^{\gamma}(\omega, T)$ by ≈10%, rather independent of the temperature or the approach (either quantum statistical or semiclassical). Due to the predominance of the polarizability contribution over the whole investigated temperature range (see table 8), the overall effect on $B_K(\omega, T)$ remains contained.

The results for the second ESHG virial coefficient of neon are collected in table 9, where both the static

Table 9. The hyperpolarizability (ESHG) second virial coefficients $B_\gamma(\lambda, T) = B_\gamma^{(0)}(\lambda, T) + 6\omega^2 B_\gamma^{(2)}(\lambda, T)$($C^4m^7J^{-3}mol^{-1} \times 10^{-68}$) and relative coefficients $b_\gamma(\lambda, T) = B_\gamma(\lambda, T)/\gamma_{||,\mathrm{ESHG}}(cm^3\,mol^{-1})$. To compute $b_\gamma(\lambda = 514.5\,nm, T)$ we have assumed $\gamma_{||,\mathrm{ESHG}} = 122.2$ au.[a]

T/K	Semiclassical			Quantum statistical		
	$B_\gamma^{(0)}(T)$	$B_\gamma^{(2)}(T)$	$b_\gamma(\lambda = 514.5\,nm, T)$	$B_\gamma^{(0)}(T)$	$B_\gamma^{(2)}(T)$	$b_\gamma(\lambda = 514.5\,nm, T)$
40.00	−11.15	−57.68	−1.820	−10.44	−50.51	−1.682
77.40	−7.78	−40.48	−1.270	−7.59	−38.16	−1.232
100.00	−7.37	−38.05	−1.202	−7.24	−36.49	−1.176
140.00	−7.22	−36.66	−1.174	−7.14	−35.70	−1.158
180.00	−7.32	−36.54	−1.186	−7.26	−35.86	−1.175
220.00	−7.50	−36.87	−1.212	−7.45	−36.35	−1.202
242.95	−7.61	−37.15	−1.229	−7.57	−36.69	−1.220
273.15	−7.77	−37.56	−1.252	−7.73	−37.17	−1.245
298.15	−7.90	−37.93	−1.271	−7.87	−37.58	−1.265
303.15	−7.93	−38.00	−1.275	−7.90	−37.66	−1.269
323.00	−8.03	−38.30	−1.291	−8.00	−37.98	−1.285
340.00	−8.12	−38.55	−1.304	−8.09	−38.26	−1.298
370.00	−8.28	−39.00	−1.327	−8.25	−38.74	−1.322
410.00	−8.47	−39.59	−1.357	−8.45	−39.36	−1.352

[a][67]. The value is 122.2 ±0.4 au.

$B_\gamma^{(0)}(T)$ and the dispersion $B_\gamma^{(2)}(T)$ contributions are included. Since in experiment it is customary to measure the pressure dependence of a gas with respect to a reference gas, it is often convenient to report a relative second virial hyperpolarizability coefficient defined as $b_\gamma(\Omega, T) = B_\gamma(\Omega, T)/\gamma(\Omega)$ (Ω is in this case $-\omega; 0, 0, \omega$). For the case of the electric field-induced second-harmonic generation we give in table 9 the coefficient $b_\gamma(\lambda = 514.5\,nm, T)$, estimated both in the semiclassical and in the quantum statistical approximations, and obtained by assuming as reference ESHG parallel component of the hyperpolarizability the experimental value of 122.2 ± 0.4 au taken from studies of Shelton and Donley [67–69] and neglecting the error bars. In figure 7, $b_\gamma(\lambda = 515.4\,nm, T)$ is plotted together with the curves of the coefficients obtained at two more wavelengths: 488 and 1024 nm (the reference values $\gamma_{||,\mathrm{ESHG}}(488.0\,nm) = 123.5 \pm 0.5$ au and $\gamma_{||,\mathrm{ESHG}}(1024\,nm) = 109.9 \pm 0.5$ au were also taken from [67–69]).

Quantum effects reduce the value of $b_\gamma(\omega, T)$ in absolute value by up to 10% around 40 K, and the effect drops to ≈1–2% at temperatures around 100 K. Around room temperature the difference between quantum statistical and semiclassical results drops to less than 0.5%, which is again comparable with the errors connected with the rather elaborate and delicate procedure which has to be adopted in the quantum calculations (see section 3.2). The frequency dispersion is far from being negligible. For a wavelength of 514.5 nm it increases the static value (in absolute value) by 20–25% in the whole range of temperatures of table 9, rather independent of the type of approach.

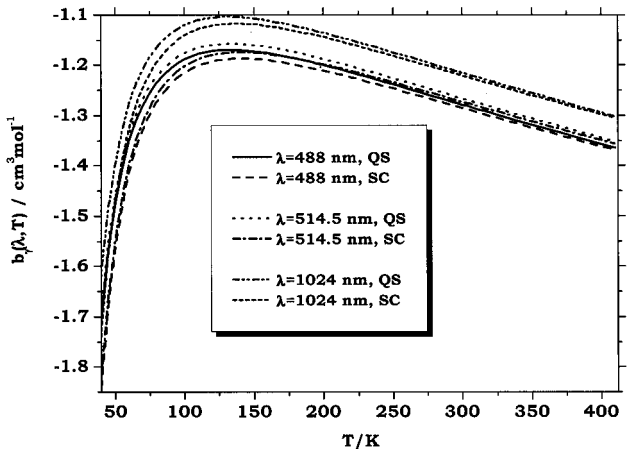


Figure 7. The relative hyperpolarizability (ESHG) second virial coefficient $b_\gamma(\omega, T) = B_\gamma(\omega, T)/\gamma_{||,\mathrm{ESHG}}(\omega)$ as a function of the temperature computed at $\lambda = 488$ nm, $\lambda = 514.5$ nm and $\lambda = 1024$ nm ($10^{-68}\,C^4\,m^7\,J^{-3}mol^{-1}$). The reference values were taken from experiment: $\gamma_{||,\mathrm{ESHG}}(\lambda = 488\,nm) = 123.5$ au [68]; $\gamma_{||,\mathrm{ESHG}}(\lambda = 514.5\,nm) = 122.2$ au [67] and $\gamma_{||,\mathrm{ESHG}}(\lambda = 1024\,nm) = 109.9$ au [69].

The values of $b_\gamma(\omega, T)$ computed for neon are of the same order of magnitude as those predicted for helium in [2], and thus they are an order of magnitude larger than predicted for argon [2].

5. Summary and conclusions

In the present work we extend our previous *ab initio* studies of the second virial coefficients for linear and nonlinear properties of helium and argon gases to neon, considered as an intermediate case as far as the binding energy of the van der Waals dimer is concerned. As shown in [4] the importance of quantum effects on the interatomic (or in general intermolecular) motion for virial coefficients depends critically on this property. Also, the evaluation of the quantum statistical expressions for the virial coefficients becomes cumbersome with increasing binding energy and the presence of an increasing number of bound and quasi-bound rovibrational states.

For the calculation of the dimer properties an approach similar to that used in [1, 2] for the Ar_2 dimer has been employed. An accurate CCSD(T) potential and CCSD interaction-induced electric dipole polarizabilities and hyperpolarizabilities have been computed, and the frequency dependence of the properties has been accounted for through second order using analytic dispersion coefficients. When comparing the interaction-induced isotropic and anisotropic polarizabilities to the previous empirical curves, we observe that the agreement is acceptable for the asymptotic long-range behaviour. It becomes rather poor at short range, where all semi-empirical models considered here fail to some extent.

The dielectric, refractivity, Kerr and hyperpolarizability second virial coefficients have been evaluated using both a semiclassical and a quantum statistical approach. It is found that for neon, quantum effects are negligible ($<$1–5%) for temperatures larger than $\approx$100 K. Only few experimental data are available for virial coefficients of electric properties of neon gas. As for argon, also for neon the experimental data on the dielectric and refractivity second virial coefficient carry at times very large uncertainties. As a consequence, and in spite of the large distribution of the experimental points, comparison between the present highly accurate *ab initio* results and experiment can only be defined as fair. A renewed effort from the experimentalists would be welcome.

The Kerr second virial coefficient of neon is dominated (contrary to what has been observed in [4] for helium) in the whole temperature range by the polarizability contribution $B_K^{\alpha}(\omega, T)$, which is approximately 30–35 times larger than the hyperpolarizability contribution at small temperatures (where quantum effects account for $\approx$10% of the coefficient) and twice to three times larger at temperatures around 400 K. The deviations from linearity in the dependence of the Kerr constant of neon on the density, not detected in the experiment of Buckingham and Dunmur [66], are thus predicted to be small but still non-negligible. The frequency dispersion of the Kerr second virial coefficient is quite contained.

The ESHG second virial coefficient of neon assumes values comparable to those computed for helium in [3], and it displays a remarkable frequency dispersion. Quantum effects are again negligible above 100 K.

This paper is dedicated to Bjoern Roos, who is responsible for the meeting of two of the authors in a memorable first edition of the *European School in Quantum Chemistry* just a few years ago. We look forward to hearing of his past, present and future contributions in the field of science for many years to come. We thank Michal Jaszuński for kindly providing detailed information on his study of the potential of Ne_2. This work has been supported by the European Research and Training Network 'Molecular Properties and Molecular Materials' (MOLPROP), Contract No. HPRN-CT-2000-00013, and by the Spanish Comisión Interministerial de Ciencia y Tecnología (PB98-0609-C04-01 Project and FP99-44446531C FPI Grant).

References

[1] Fernández, B., Hättig, C., Koch, H., and Rizzo, A., 1999, *J. chem. Phys.*, **110,** 2872.
[2] Hättig, C., Larsen, H., Olsen, J., Jørgensen, P., Koch, H., Fernández, B., and Rizzo, A., 1999, *J. chem. Phys.*, **111,** 10099.
[3] Koch, H., Hättig, C., Larsen, H., Olsen, J., Jørgensen, P., Fernández, B., and Rizzo, A., 1999, *J. chem. Phys.*, **111,** 10108.
[4] Rizzo, A., Hättig, C., Fernández, B., and Koch, H., 2002, *J. chem. Phys.*, **117,** 1234.
[5] Pecul, M., and Rizzo, A., 2002, *Molec. Phys.*, **100,** 447.
[6] Rizzo, A., Ruud, K., and Bishop, D. M., 2002, *Molec. Phys.*, **100,** 799.
[7] Buckingham, A. D., and Pople, J. A., 1956, *Faraday Discuss. chem. Soc.*, **22,** 17.
[8] Moldover, M. R., and Buckley, T. J., 2001, *Int. J. Thermophys.*, **22,** 859.
[9] Moldover, M. R., 1998, *J. Res. Natl. Inst. Stand. Technol.*, **103,** 167.
[10] Moszynski, R., Heijmen, T. G. A., Wormer, P. E. S., and van der Avoird, A., 1996, *J. chem. Phys.*, **104,** 6997.
[11] Moszynski, R., Heijmen, T. G. A., and van der Avoird, A., 1995, *Chem. Phys. Lett.*, **247,** 440.
[12] Gibbons, R. M., 1969, *Cryogenics*, **9,** 251.
[13] Dymond, J. H., and Smith, E. B., 1969, *The Virial Coefficients of Gases: A Critical Compilation* (Oxford: Clarendon Press).
[14] Eggenberger, R., Gerber, S., Huber, H., Searles, D., and Welker, M., 1993, *J. chem. Phys.*, **99,** 9163.
[15] Frommhold, L., and Proffitt, M. H., 1980, *Phys. Rev.* A, **21,** 1249.
[16] Kress, J. W., and Kozak, J. J., 1977, *J. chem. Phys.*, **66,** 4516.
[17] Dacre, P. D., 1981, *Can. J. Phys.*, **59,** 1439.
[18] Dacre, P. D., 1982, *Can. J. Phys.*, **60,** 963.
[19] Meinander, N., Tabisz, G. C., and Zoppi, M., 1986, *J. chem. Phys.*, **84,** 3005.

[20] CECCHERINI, S., MORALDI, M., and FROMMHOLD, L., 1999, *J. chem. Phys.*, **111,** 6316.
[21] MAROULIS, G., 2000, *J. phys. Chem.* A, **104,** 4772.
[22] MAROULIS, G., and HASKOPOULOS, A., 2002, *Chem. Phys. Lett.*, **358,** 64.
[23] ORCUTT, R. H., and COLE, R. H., 1966, *J. chem. Phys.*, **46,** 697.
[24] VIDAL, D., and LALLEMAND, M., 1976, *J. chem. Phys.*, **64,** 4293.
[25] HUOT, J., and BOSE, T. K., 1991, *J. chem. Phys.*, **95,** 2683.
[26] BULANIN, M. O., HOHM, U., LADVISHCHENKO, Y. M., and KERL, K., 1994, *Z. Naturforsch.*, **49a,** 890.
[27] MEINANDER, N., 1994, *Chem. Phys. Lett.*, **228,** 295.
[28] BURNS, R. C., GRAHAM, C., and WELLER, A. R. M., 1986, *Molec. Phys.*, **59,** 41.
[29] ACHTERMANN, H. J., HONG, J. G., MAGNUS, G., AZIZ, R. A., and SLAMAN, M. J., 1993, *J. chem. Phys.*, **98,** 2308.
[30] BOYS, S. F., and BERNARDI, F., 1970, *Molec. Phys.*, **19,** 553.
[31] AZIZ, R. A., and SLAMAN, M. J., 1989, *Chem. Phys.*, **130,** 187.
[32] BURDA, J. V., ZAHRADNIK, R., HOBZA, P., and URBAN, M., 1990, *Molec. Phys.*, **89,** 425.
[33] CYBULSKI, S. M., and TOCZYLOWSKI, R. R., 1999, *J. chem. Phys.*, **111,** 10520.
[34] VAN MOURIK, T., and VAN LENTHE, J. H., 1995, *J. chem. Phys.*, **102,** 7479.
[35] GDANITZ, R. J., 2001, *Chem. Phys. Lett.*, **348,** 67.
[36] DUNNING, T. H., 1989, *J. chem. Phys.*, **90,** 1007.
[37] KENDALL, R. A., DUNNING, T. H., and HARRISON, R. J., 1992, *J. chem. Phys.*, **96,** 6796.
[38] WOON, D. E., and DUNNING, T. H., 1993, *J. chem. Phys.*, **98,** 1358.
[39] WOON, D. E., and DUNNING, T. H., 1994, *J. chem. Phys.*, **100,** 2975.
[40] WOON, D. E., and DUNNING, T. H., 1995, *J. chem. Phys.*, **103,** 4572. The basis sets were obtained from the Extensible Computational Chemistry Environment Basis Set Database, Version 1.0, as developed and distributed by the Molecular Science Computing Facility, Environmental and Molecular Sciences Laboratory which is part of the Pacific Northwest Laboratory, PO Box 999, Richland, Washington 99352, USA, and funded by the US Department of Energy. PNL is a multiprogram laboratory operated by Batelle Memorial Institute for the US Department of Energy under contract DE-AC06-76RLO 1830.
[41] KOCH, H., CHRISTIANSEN, O., KOBAYASHI, R., JØRGENSEN, P., and HELGAKER, T., 1994, *Chem. Phys. Lett.*, **228,** 233.
[42] KOCH, H., DE MERÁS, A. S., HELGAKER, T., and CHRISTIANSEN, O., 1996, *J. chem. Phys.*, **104,** 4157.
[43] HELGAKER, T., JENSEN, H. J. Å., JØRGENSEN, P., OLSEN, J., RUUD, K., ÅGREN, H., AUER, A. A., BAK, K. L., BAKKEN, V., CHRISTIANSEN, O., CORIANI, S., DAHLE, P., DALSKOV, E. K., ENEVOLDSEN, T., FERNÁNDEZ, B., HÄTTIG, C., HALD, K., HALKIER, A., HEIBERG, H., HETTEMA, H., JONSSON, D., KIRPEKAR, S., KOBAYASHI, R., KOCH, H., MIKKELSEN, K. V., NORMAN, P., PACKER, M. J., PEDERSEN, T. B., RUDEN, T. A., SANCHEZ, A., SAUE, T., SAUER, S. P. A., SCHIMMELPFENNIG, B., SYLVESTER-HVID, K. O., TAYLOR, P., and VAHTRAS, O., 2001, Dalton—an electronic structure program, release 1.2. See http://kjemi.uio.no/software/dalton/dalton.html
[44] HALKIER, A., KIRCHNER, B., HUBER, H., and JASZUŃSKI, M., 2000, *Chem. Phys.*, **253,** 183.
[45] AZIZ, R. A., JANZEN, A. R., and MOLDOVER, M. R., 1995, *Phys. Rev. Lett.*, **74,** 1586.
[46] CHRISTIANSEN, O., HALKIER, A., KOCH, H., JØRGENSEN, P., and HELGAKER, T., 1998, *J. chem. Phys.*, **108,** 2801.
[47] HÄTTIG, C., CHRISTIANSEN, O., and JØRGENSEN, P., 1997, *J. chem. Phys.*, **107,** 10592.
[48] HÄTTIG, C., CHRISTIANSEN, O., and JØRGENSEN, P., 1998, *Chem. Phys. Lett.*, **282,** 139.
[49] HÄTTIG, C., and JØRGENSEN, P., 1999, *Adv. quantum Chem.*, **35,** 111.
[50] TAO, F. M., and PAN, Y. K., 1994, *Molec. Phys.*, **81,** 507.
[51] TAO, F. M., 1994, *J. chem. Phys.*, **100,** 3645.
[52] HÄTTIG, C., and JØRGENSEN, P., 1998, *J. chem. Phys.*, **106,** 2762.
[53] BUCKINGHAM, A. D., and POPLE, J. A., 1955, *Trans. Faraday Soc.*, **51,** 1029.
[54] DONLEY, E. A., and SHELTON, D. P., 1993, *Chem. Phys. Lett.*, **215,** 156.
[55] MOSZYNSKI, R., 1997, Habilitation Thesis, University of Warsaw, Poland.
[56] DE BOER, J., 1949, *Rep. Prog. Phys.*, **12,** 305.
[57] HÄTTIG, C., MOSZYNSKI, R., and RIZZO, A., 2003, to be published.
[58] FALK, H., and BRUCH, L. W., 1969, *Phys. Rev.*, **180,** 442.
[59] LE ROY, R. J., KLEIN, M. L., and MCGEE, I. J., 1974, *Molec. Phys.*, **28,** 587.
[60] TANAKA, Y., and YOSHINO, K., 1972, *J. chem. Phys.*, **57,** 2964.
[61] MILLS, I., CVITAS, T., HOMANN, K., KALLAY, N., and KUCHITZU, K., 1993, *Quantities, Units and Symbols in Physical Chemistry* (Oxford: Blackwell Science).
[62] CACELLI, I., RIZZO, A., and HÄTTIG, C., *KORG, a program for the solution of the radial Schrödinger equation for bound and discrete levels.*
[63] BUCKINGHAM, A. D., and GRAHAM, C., 1974, *Proc. R. Soc. London Ser.* A, **336,** 275.
[64] ORCUTT, R. H., and COLE, R. H., 1967, *J. chem. Phys.*, **46,** 697.
[65] LALLEMAND, M., and VIDAL, D., 1977, *J. chem. Phys.*, **66,** 4776.
[66] BUCKINGHAM, A. D., and DUNMUR, D. A., 1968, *Trans. Faraday Soc.*, **64,** 1776.
[67] SHELTON, D. P., 1990, *Phys. Rev.* A, **42,** 2578.
[68] SHELTON, D. P., 1989, *Phys. Rev. Lett.*, **62,** 2660.
[69] SHELTON, D. P., and DONLEY, E. A., 1992, *Chem. Phys. Lett.*, **195,** 591.